Published online 22 November 2017 *Nucleic Acids Research, 2017, Vol. 45, No. 22* ***12625–12637***
doi: 10.1093/nar/gkx1128

SURVEY AND SUMMARY

Meta-analysis of DNA double-strand break response kinetics

Jakub A. Kochan[1,†], Emilie C.B. Desclos[1,†], Ruben Bosch[1], Luna Meister[1], Lianne E.M. Vriend[1], Haico van Attikum[2] and Przemek M. Krawczyk[1,*]

[1]Department of Medical Biology and Laboratory of Experimental Oncology and Radiobiology (LEXOR), Cancer Center Amsterdam, Academic Medical Center, Meibergdreef 15, 1105 AZ Amsterdam, The Netherlands and [2]Department of Human Genetics, Leiden University Medical Center, Einthovenweg 20, 2333 ZC Leiden, The Netherlands

Received August 04, 2017; Revised October 24, 2017; Editorial Decision October 25, 2017; Accepted November 13, 2017

ABSTRACT

Most proteins involved in the DNA double-strand break response (DSBR) accumulate at the damage sites, where they perform functions related to damage signaling, chromatin remodeling and repair. Over the last two decades, studying the accumulation of many DSBR proteins provided information about their functionality and underlying mechanisms of action. However, comparison and systemic interpretation of these data is challenging due to their scattered nature and differing experimental approaches. Here, we extracted, analyzed and compared the available results describing accumulation of 79 DSBR proteins at sites of DNA damage, which can be further explored using *Cumulus* (http://www.dna-repair.live/cumulus/)—the accompanying interactive online application. Despite large inter-study variability, our analysis revealed that the accumulation of most proteins starts immediately after damage induction, occurs in parallel and peaks within 15–20 min. Various DSBR pathways are characterized by distinct accumulation kinetics with major non-homologous end joining proteins being generally faster than those involved in homologous recombination, and signaling and chromatin remodeling factors accumulating with varying speeds. Our meta-analysis provides, for the first time, comprehensive overview of the temporal organization of the DSBR in mammalian cells and could serve as a reference for future mechanistic studies of this complex process.

INTRODUCTION

Among the various types of lesions that daily threaten the integrity of mammalian genomes, DNA double-strand breaks (DSBs) are arguably the most dangerous, since even a single unrepaired DSB can lead to potentially cytotoxic or oncogenic chromosome rearrangements. To counteract these lesions, mammalian cells have evolved a sophisticated DSB response (DSBR) network, requiring the concerted action of dozens of proteins.

The mammalian response to DSBs involves (i) the detection of lesions, (ii) amplification (signaling) of the damage signal, (iii) activation of checkpoints that globally affect cell cycle and metabolism, (iv) remodeling of the DSB-flanking chromatin environment to initiate, facilitate and modulate the assembly of multi-protein complexes (1–3) and finally (v) repair, accomplished by two major, mechanistically distinct pathways—homologous recombination (HR) (4) and non-homologous end joining (NHEJ) (5). The latter mechanism has been subdivided into the complementary, but mechanistically distinct, classical and alternative sub-pathways (5).

Most DSBR factors accumulate at or in the vicinity of DSB sites, forming cytologically discernible foci and dissociate after repair is completed. The function and spatial organization of these dynamic structures is not completely understood, but by visualizing and quantifying their assembly and disassembly it is possible to indirectly monitor repair processes. Moreover, when a high concentration of DNA damage is induced in a restricted area of the nucleus, by so-called microirradiation, it is possible to visualize and analyze the accumulation of fluorescently tagged DSBR factors at the damaged area in real-time (6). The (changes in) kinetic behavior of DSBR factors in response to DSBs can

*To whom correspondence should be addressed. Tel: +31 205 668 746; Fax: +31 206 974 156; Email: p.krawczyk@amc.uva.nl
†These authors contributed equally to the paper as first authors.

provide valuable information on their involvement in various repair pathways, their interactions with other proteins and the spatio-temporal organization of DSBR in general.

Numerous microirradiation methods have been developed to locally induce DNA damage. Continuous and pulsed lasers with wavelengths ranging from ultraviolet (UV)-B to infrared have been used for this purpose either with or without presensitization with halogenated nucleoside analogs like BrdU or DNA-binding dyes like Hoechst (6,7). Laser-based approaches induce a wide and poorly characterized range of DNA-damage types, including interstrand crosslinks, 6–4 photoproducts, pyrimidine dimers, abnormal nucleotide modifications, such as oxidation, deamination, or methylation, and single- and double-strand breaks (8,9). Microirradiation using ultra-soft X-rays (10–12), α-particles (13) or heavy ion beams (14,15) has also been used to study DSBR in living cells. In contrast to lasers, ionizing radiation mostly induces single- and double-strand breaks (16), but the complexity of these breaks increases with linear energy transfer of the used radiation type (17).

All these methods have been applied to visualize and quantify accumulation of dozens of DSBR proteins at damage sites. Some of them have been analyzed in multiple studies, often by independent groups. Systematic interpretation of these data might provide insights into DSB repair kinetics that could be correlated with other biochemical and molecular end points and with the known models of DSBR. However, to our knowledge, such a comprehensive analysis has not yet been attempted.

Here, we explored >100 different studies that present data on the accumulation of 79 DSBR-related proteins at DNA-damage sites. We extracted, aggregated, normalized and systematically analyzed these data to determine the kinetic parameters governing the assembly of the DSBR machinery. The results of our analysis provide a global perspective on the timing and sequence of DSBR events in mammalian cells.

MATERIALS AND METHODS

Data extraction, processing and analysis

The data extraction and processing strategy is depicted schematically in Figure 1. Two publicly available databases (Google Scholar and PubMed) were queried using various combinations of names of proteins related to DSBR and terms 'repair', 'radiation', 'microirradiation', 'laser' and 'accumulation'. The retrieved articles were scanned for graphs quantifying the accumulation of fluorescently tagged DNA repair proteins at microirradiated sites (i.e. the relationship between fluorescence intensity at the damaged site and time after microirradiation) in living cells. We considered the graphs as suitable for further analysis if (1) the duration of imaging was sufficient for the fluorescence intensity to (nearly) reach a plateau and (2) at least four measurement points were available before the fluorescence intensity reached the plateau. Data were extracted from the graphs using the openly accessible WebPlotDigitizer (http://arohatgi.info/WebPlotDigitizer/app). Additionally, metadata describing relevant experimental parameters were extracted from the articles (Supplementary Dataset S1). The extracted data were then processed using a custom-written Matlab script in the following steps (Figure 1D and Supplementary Figure S1):

(i) Time data were converted to seconds.
(ii) To compare accumulation kinetics between studies, the lower bound of all intensity data was first normalized to 0 in the following way:
  (a) In the majority of cases, the original data appeared to have already been normalized to fluorescence intensity (I) measured immediately after damage induction and accumulation (fluorescence intensity increase) was apparent already at the next time point, t_1, so that $I_1 > I_0$. In those cases, the reported fluorescence intensity at the initial time point (I_0) was subtracted from all intensity data, resulting in the lower bound normalized to 0.
  (b) In some cases, the fluorescence intensity immediately after damage induction was *lower* than at t_0 ($I_1 < I_0$), only to rapidly increase at subsequent time point(s). This is generally caused by photobleaching of the fluorescent tag by laser microirradiation and was not observed when DNA damage was induced, for instance, by ionizing radiation. The ensuing rapid fluorescence increase at subsequent time points is a product of two processes: (1) redistribution of non-bleached proteins from the areas surrounding the microirradiated site; (2) accumulation of proteins at the damage site. Since the speed of the redistribution is dependent on the unknown diffusion speed of each protein, it is not feasible to calculate the contribution of the two processes to the initial fluorescence increase after photobleaching. To normalize data from these experiments, we thus divided all intensity data by the lowest reported relative intensity value. Subsequently, we (1) removed all data points prior to the time when this lowest intensity was reached and (2) subtracted the time required to reach this point from all remaining time data points.
(iii) Next, we normalized the upper bound of all intensity data to 1. Since not all analyzed studies allowed the accumulation to reach the saturation (plateau) phase, direct normalization of the upper bound of data obtained from such 'prematurely terminated' experiments (by dividing all intensity values by the maximum intensity reached, I_{MAX}) would affect the normalized accumulation kinetics. Therefore, the data were first fitted with a theoretical curve in the form of $f_{(t)} = (1-\exp(-t / \tau)) \times n$ (18), after which all intensity values were divided by the normalization parameter n. This produced normalized data that would be upper-bounded by 1 if plateau would have been reached.
(iv) In some analyzed cases, the start of accumulation was delayed (see for instance 53BP1 in Figure 3B), resulting in sub-optimal fits of the first-order exponential equation. One potential solution is to apply a second-order equation (18). However, because the number of such cases was limited, and because the time resolution of datasets was often not sufficient for such fitting, we instead iteratively determined the relative delay of accu-

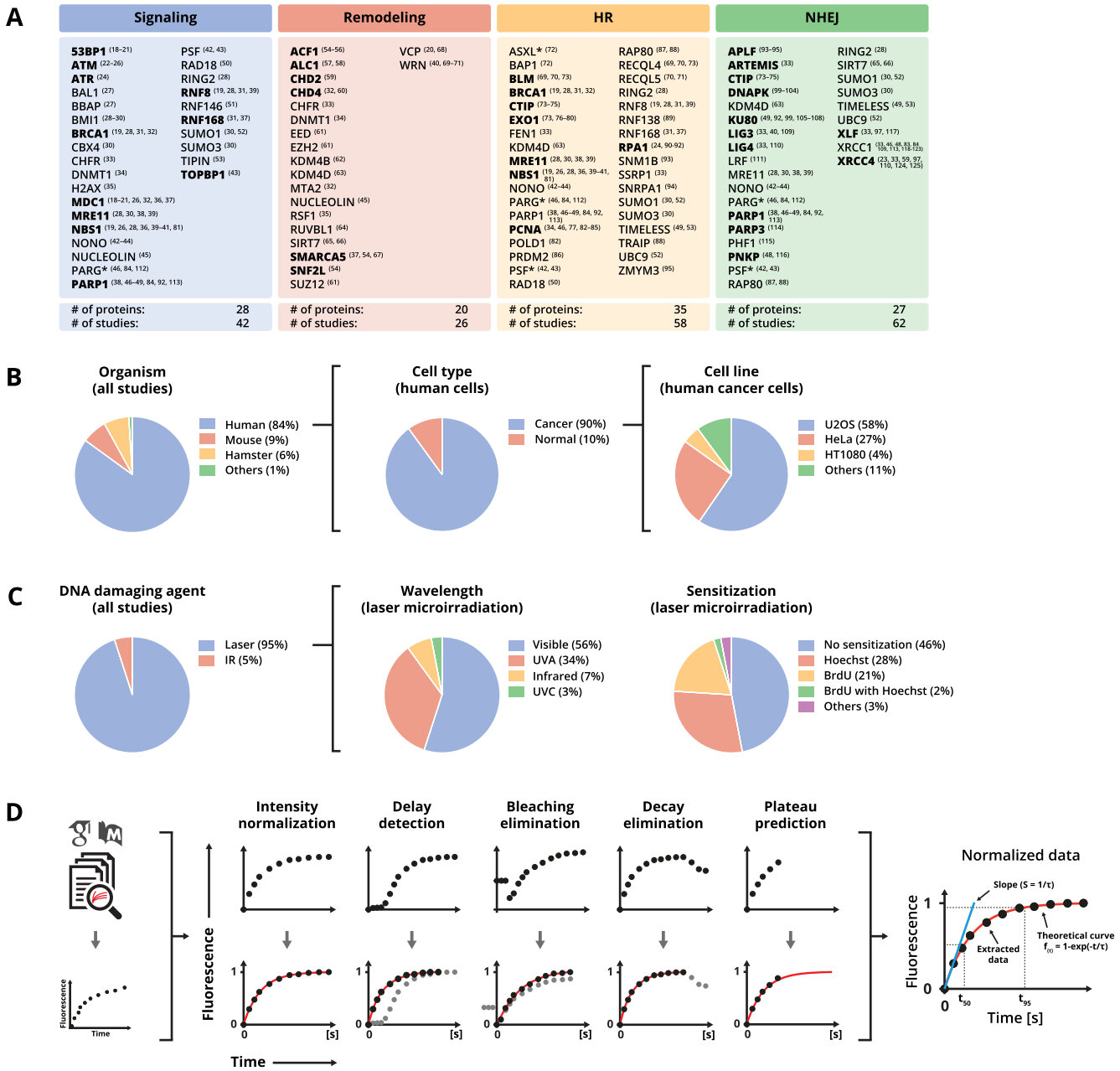

Figure 1. Overview of the data analyzed in this study. (**A**) A table listing all analyzed proteins, ordered per pathway. References to studies that analyzed each individual protein are indicated in brackets. Core factors of each pathway are marked in bold. (**B** and **C**) Statistical overview of the analyzed data, showing the origin, type and line of cells used in the studies (B) and the applied DNA-damage induction methods (C). (**D**) Schematic overview of the data processing procedures. See the 'Materials and Methods' section for detailed description. * The involvement of these proteins in the indicated DSBR pathways is not well documented in the available literature.

mulation by shifting the time component of the data until a maximal goodness of fit (R^2) was obtained using the first-order equation. Such iteratively obtained fit was better than a fit of a second-order equation in nearly all cases (not shown).

(v) After normalization, a single theoretical first-order exponential equation $f_{(t)} = 1\text{-}\exp(-t / \tau)$ could be fitted to all data. The accumulation speed was defined as the slope of the initial (linear) part of the fitted curve ($S = 1 / \tau$). We also calculated the time required for the normalized fluorescence intensity to reach 50% and 95% of its maximal value (t_{50} and t_{95}, respectively). In the cases where accumulation was delayed (see step 4), the measured delay was added to the value of t_{50} and t_{95} that were calculated from the fit.

RESULTS

Accumulation of DSBR factors at damage sites has mostly been studied using laser microirradiation and two human cancer cell lines

Our literature search returned 108 studies (18–125) in which the accumulation of 79 individual proteins was quantified in 250 datasets (Figure 1A). Of these studies 84% were performed using cells of human origin, while the remaining focused on mouse (9%) or hamster cell lines (6%) (Figure 1B). Of all analyses performed in human cells, 90% used cancer cells. Of these, U2OS and HeLa represented 85% of cases (58% and 27%, respectively).

In the vast majority of all analyzed studies (95%) various laser microirradiation techniques were applied to induce DNA damage (Figure 1C). Of these, the most frequently used (93%) were laser sources of visible and ultraviolet (UV) light (UVA and UVC), while the other 7% of studies applied infrared lasers. In 54% of these studies, nucleoside analogs (BrdU), DNA-binding dyes (Hoechst) or their combination (7) were additionally used to enhance damage induction. In the remaining reports, DNA damage was induced using sophisticated particle accelerator installations. In summary, the majority of available data on the accumulation of DSBR proteins at DNA-damage sites have been obtained using only two human cancer cell lines (HeLa and U2OS) and laser microirradiation, often in the presence of sensitizers, to induce DNA damage.

Online interactive application for visualization and analysis of accumulation data

To facilitate analysis of accumulation data presented in this study, we created an openly accessible website (www.dna-repair.live/cumulus) (Figure 2), where the results of our analysis can be interactively studied and visualized. The web interface allows the analysis of accumulation data per protein, per study or per dataset. Additionally, it is possible to visualize a number of parameters simultaneously for all proteins or for a selected subset of proteins (e.g. those involved in a single repair pathway) or studies (e.g. those using human cells). The website is periodically updated as new accumulation data become available. Any data submitted by investigators (submission instructions can be found on the website) will also be added to the online database, enabling comparisons between newly generated and existing data. All data used in this study can be downloaded from the website and are additionally included in Supplementary Materials (Supplementary Dataset S1).

The accumulation kinetics of most DNA repair proteins at damage sites follows a similar exponential trajectory

To determine the parameters describing the kinetics of accumulation of proteins at DNA-damage sites, we fitted curves given by first and second-order exponential equations (18) to the extracted data showing changes in fluorescence intensity (due to accumulation of fluorescently tagged DSBR proteins) at damaged sites over time. In nearly all cases, a better fit was obtained when using the first-order equation: $f_{(t)} = 1\text{-}\exp(-t / \tau)$. Accordingly, the average cumulative goodness of first-order fit (expressed by R^2) was much higher than that of second-order fit (not shown). Even in cases when second-order equation provided a better fit, the goodness of fit did not differ substantially between the first and second-order equations (not shown). We therefore choose the first-order equation for further analysis of all data.

The kinetics of accumulation of most DSBR proteins shows considerable inter-study variation

To compare the accumulation kinetics of individual proteins, we used the parameters derived from the fitted exponential equations to calculate, from each study, the time required for the accumulation of each protein to reach 50% (t_{50}, Figure 3A) or 95% (t_{95}, Supplementary Figure S2) of its maximum, as well as the slope of the initial, linear part of the fitted curve ($S = 1 / \tau$, Supplementary Figure S3). The latter parameter is independent of the delay in accumulation initiation that was reported in a number of studies, while t_{50} and t_{95} incorporate this delay (see 'Materials and Methods' section for detailed description of data processing). In cases where multiple datasets describing accumulation of a single protein were available in a single study, we first calculated the mean slope, t_{50} and t_{95} from all these datasets. Next, we determined, for each protein, the median t_{50} and t_{95} derived from all studies that reported data for this particular protein. When we ordered these median t_{50} and t_{95} values and slope for all proteins, (Figure 3A; Supplementary Figures S2 and 3), we made a number of striking observations. First, half of all proteins reached 50% of maximal accumulation in under 30 s and all proteins within 10 min. Second, near-complete accumulation was reached by half of all proteins in under 2 min and by nearly all proteins (90%) within ∼8 min. In the remaining 10% of cases, full accumulation was achieved within 45 min. Third, in cases when multiple studies reported data on a given protein, we generally observed a considerable discrepancy between t_{50} and t_{95} values derived from different studies.

To further explore the latter observation, we selected a number of proteins that had been analyzed in multiple studies for closer inspection. For some of these proteins, the inter-study variability appeared to be relatively small (Figure 3B). For instance, for APLF and 53BP1, some studies reported a delayed initiation of accumulation, while in most studies the accumulation started immediately after damage induction. In the case of APLF, laser microirradiation was applied by all studies, but results of one of them show delayed accumulation. In the case of 53BP1, the delayed accumulation was reported in a study that used heavy ions to induce DNA damage, while in studies based on laser microirradiation the accumulation appeared to start without delay. For CtBP-interacting protein (CTIP), one of the studies reported a fast accumulation ($t_{50} = \sim$5 s) that differed dramatically from that reported by two other studies ($t_{50} = \sim$300–400 s). Interestingly, all three studies were performed in U2OS cells, but using laser microirradiation with differing laser wavelengths and presensitization methods. The accumulation of BRCA1 reported in a study using mouse embryonic fibroblasts and two-photon laser microirradiation

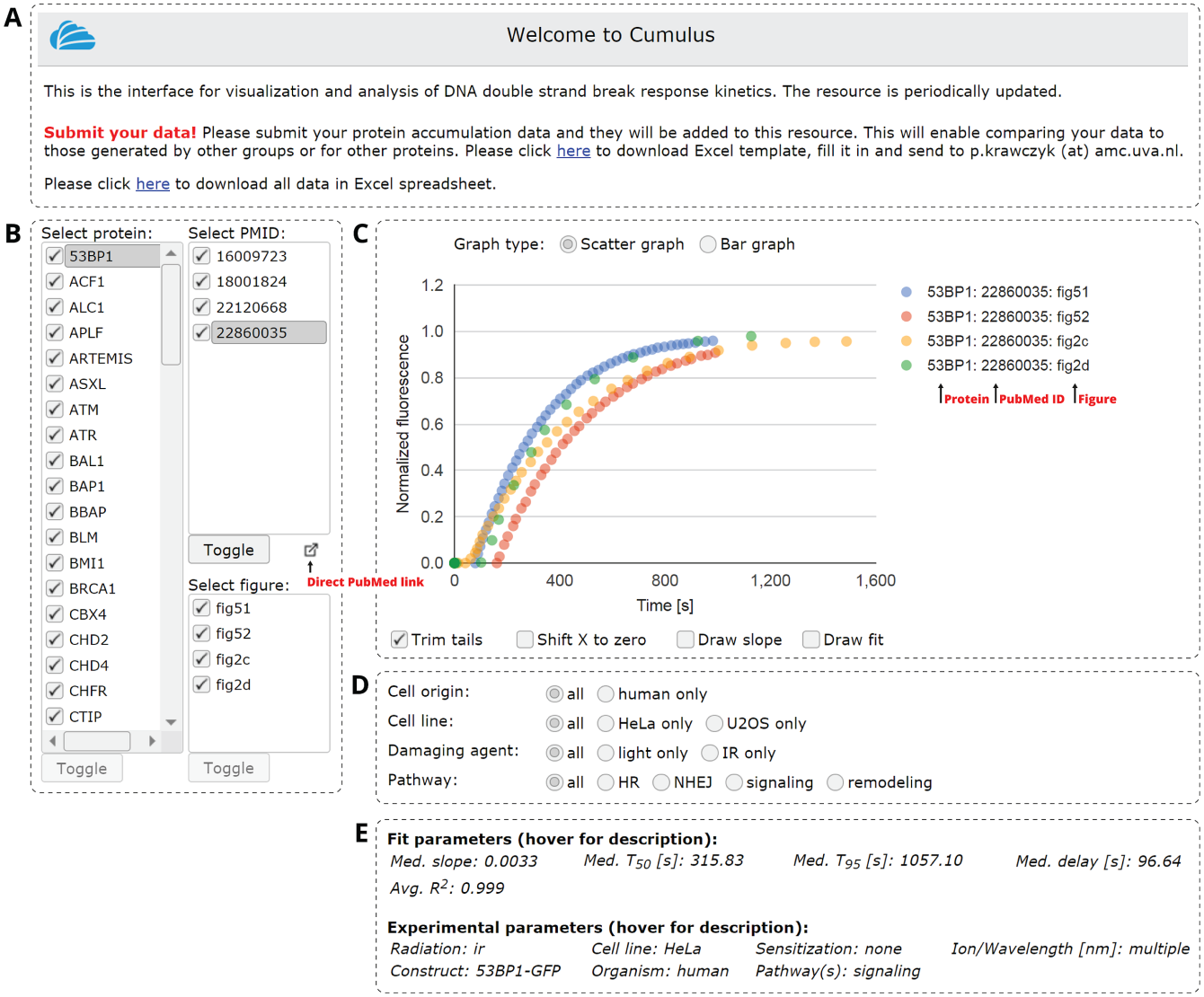

Figure 2. Overview of the interactive web interface for visualization and analysis of accumulation. (**A**) Data upload/download panel. (**B**) List of all analyzed proteins, of all studies that analyzed each protein (identified by their Pubmed ID) and of all datasets (figures) in each study from where accumulation data were extracted. (**C**) Data visualization panel. The normalized data can be be visualized either directly or as a bar graph showing a number of parameters (t_{50}, t_{95}, slope) for each protein. (**D**) The data can be filtered using the indicated parameters. (**E**) Panel displaying various parameters of the selected protein/study/dataset and of the exponential fit.

was dramatically faster than in three other studies that used the human U2OS cancer cells (t_{50} = ~25 s versus ~250–340 s). For the exonuclease EXO1, t_{50} ranged between ~2 and 80 s. In the case of MRE11, accumulation reported in one study differed considerably from that in three other studies (t_{50} = ~140 s versus ~14–30 s). In contrast to BRCA1, however, the kinetics reported in mouse embryonic fibroblasts was similar to that in U2OS cells. For XRCC1, varying accumulation speeds have been reported (t_{50} = ~4–180 s), with two studies in hamster cells showing relatively fast kinetics (t_{50} = 15–31 s), similar to a number of studies in human cells.

For a more general illustration of variation in the reported accumulation data, we analyzed the distribution of t_{50} values for proteins included in at least two independent studies. We found a relatively large normalized standard deviation of t_{50} values (59% of the mean) obtained from the individual studies. Thus, while our analysis shows that the accumulation data are robust for many DSBR proteins, it also reveals considerable inter-study variation for some of these factors.

DSBR pathways are characterized by distinct accumulation kinetics

To attain a broader perspective on the temporal organization of DSBR, we assigned all proteins to four categories: (i) signaling, (ii) chromatin remodeling, (iii) HR and (iv) NHEJ (Figure 1A) (2,3,126–128). Further, for each pathway we selected a number of 'core' factors (marked in bold in Figure 1A), on the basis of their known importance for the functioning of these pathways. A number of proteins (e.g. PARP1, MRE11, NBS1 and BRCA1) were assigned

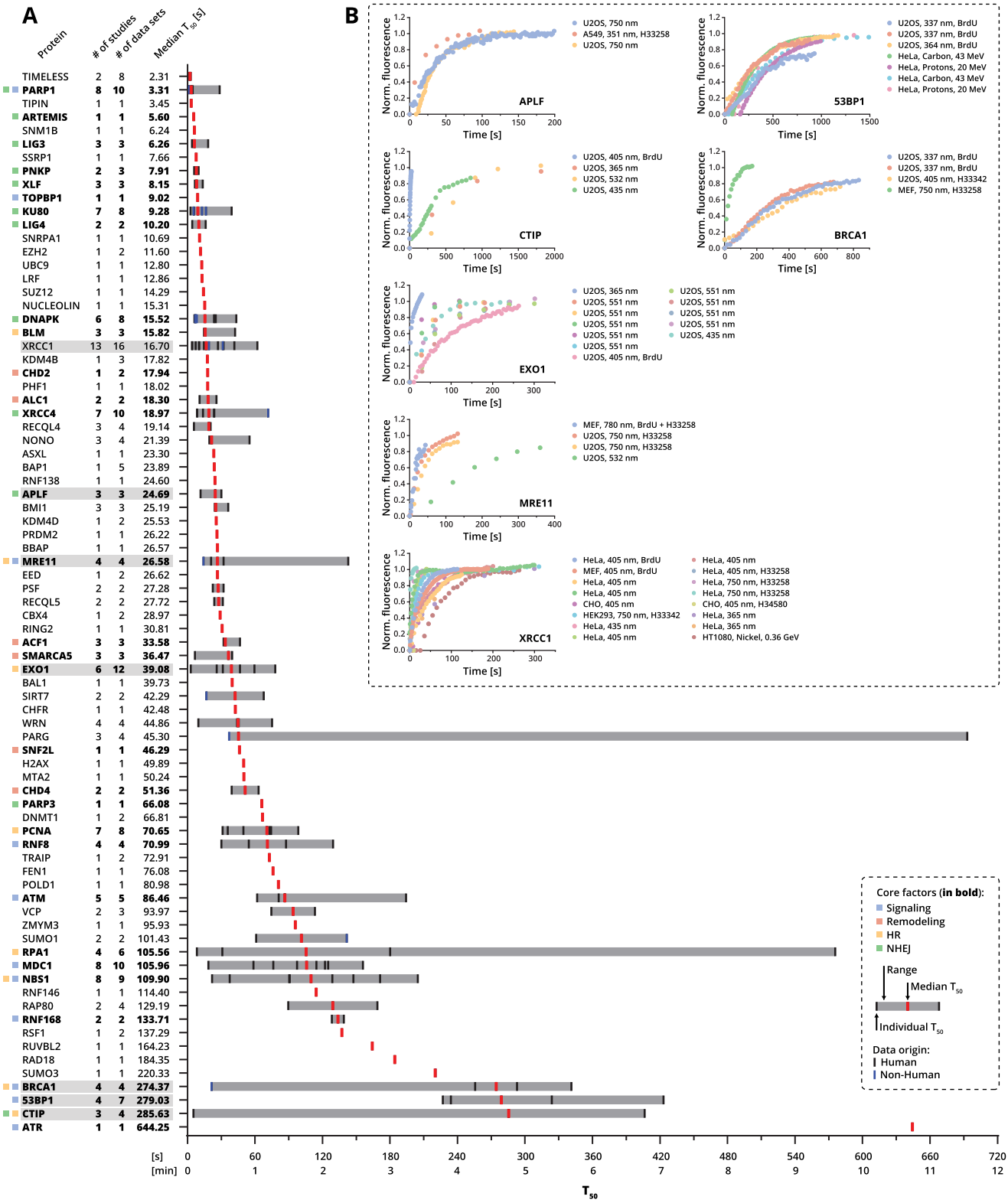

Figure 3. DSBR proteins are characterized by varying accumulation speeds. (**A**) Accumulation speed, represented as t_{50}, of all proteins analyzed in this study. The colored squares indicate the involvement of each protein in the indicated DSBR pathways. Core factors are indicated in bold. Black and blue vertical lines indicate datasets originating from studies in human or non-human cells, respectively. Red vertical lines indicate the median t_{50} value for each protein, calculated from all studies that analyzed this protein. (**B**) Example of normalized accumulation data, with cell line and irradiation parameters indicated in the legend of each graph.

to multiple categories, reflecting their reported involvement in multiple aspects of DNA repair. We then calculated the mean t_{50} of all core factors involved in each pathway (Figure 4). Results revealed NHEJ proteins as the fastest of the DSBR machinery, with the median t_{50} of core factors ∼10 s. Core HR and chromatin remodeling factors were generally slower (median t_{50} = ∼95 and 35 s, respectively). The accumulation of some HR factors (RPA1, BRCA1 and CTIP) was slow, but results also showed a considerable inter-study variation, with t_{50} values differing by nearly 20-fold for RPA1 and by ∼80-fold for CTIP (see also the previous section). Proteins involved in DNA-damage signaling showed a wide range of accumulation speeds, from the extremely fast PARP1 (t_{50} = ∼2 s) to the relatively slow 53BP1 (t_{50} = ∼10 min).

Reconstructing the sequence of DSBR events from the accumulation kinetics

The timing of arrival of proteins to DNA-damage sites should, in principle, reflect their sequential position in the underlying mechanism. We therefore attempted to reconstruct the sequence of events in the various DSBR pathways from the accumulation speed of proteins involved in these pathways, and compared it to the generally accepted models of DNA repair.

PARP1 is considered to be among the first proteins to arrive at the sites of multiple damage types, temporarily marking itself and surrounding chromatin with poly(ADP)ribose chains which, in turn, attract multiple downstream factors, including those involved in single-strand break response and DSBR. The signaling triggered by DSBs specifically involves the MRE11/RAD50/NBS1 (MRN) complex, which activates the Ataxia telangiectasia mutated (ATM) kinase upon its recruitment to DSBs. ATM phosphorylates a number of targets, including MDC1, promoting its retention in the vicinity of DSBs. Phosphorylated MDC1 attracts RNF8 and RNF168, which coordinate a ubiquitination cascade that promotes recruitment of 53BP1 and BRCA1 (31,129). This sequence of events is generally reflected by the accumulation kinetics of involved proteins, with the exception of RNF8 which appears to accumulate faster than ATM, MDC1 and NBS1. Surprisingly, MRE11 and NBS1 appeared to accumulate with clearly distinct kinetics (t_{50} = ∼25 and 130 s, respectively), even though these proteins are considered to operate in a single complex.

Classical NHEJ (c-NHEJ) is initiated by the KU heterodimer which, together with DNA-PKcs, binds and likely tethers the broken DNA ends (126,130). This is followed by end processing, either by KU itself (131,132) or by accessory proteins, including the MRN complex, Werner syndrome ATP-dependent helicase (WRN), Bifunctional polynucleotide phosphatase/kinase (PNKP), Aprataxin and PNK-like factor (APLF), Aprataxin (APTX) and Artemis. The rejoining of processed ends is accomplished by the XRCC4/LigIV complex, with help of XLF and PAXX (133). Alternative NHEJ (alt-NHEJ) pathway is promoted by the MRN complex and CTIP and mediated by WRN, PARP1 and LIG1 or LIG3/XRCC1 (134). The accumulation-based sequence of c-NHEJ events does not seem to recapitulate this consensus mechanistic model, since Artemis, PNKP and XLF accumulated slightly faster than KU and LIG4, which were closely followed by DNA-PK, XRCC4 and APLF. However, it should be noted that differences in accumulation speed of all these factors were relatively small. The accumulation speed of factors involved in alt-NHEJ (PARP1, XRCC1, LIG3 and PNKP) was comparable to that of c-NHEJ factors, with accumulation of PARP1 closely followed by LIG3, PNKP and XRCC1.

Early steps of HR involve 5′ to 3′ resection of the DNA ends, initiated by the MRN complex and CTIP, extended by EXO1 and DNA2 and promoted by BRCA1 (135). The 3′ single-stranded DNA overhangs are then rapidly coated by RPA, which is subsequently replaced by RAD51, with mediation of BRCA2. The RAD51 nucleoprotein filaments control the search for the homologous DNA and invasion of the 3′ overhangs into the template strand. DNA polymerases then copy the missing sequence from the template and after resolution of the heteroduplexes any remaining DNA flaps are removed and gaps filled. Of the few core HR factors whose accumulation has been quantified, BLM and EXO1 were first to arrive at microirradiated sites, with PCNA (considered to control the fate of stalled replication forks), RPA1 and BRCA1 following suit. Surprisingly, with median t_{50} = ∼300 s, CTIP appears to be the slowest of core HR factors, although one study did report a very fast accumulation of this protein. It is unclear whether these observations reflect experimental variability or participation of CTIP in early and late steps of HR which could depend on the type of induced DNA lesions.

DSB-induced chromatin remodeling involves changes in chromatin composition and organization, as well as a plethora of protein post-translational modifications, to facilitate and/or regulate repair and signaling activities. Therefore, remodeling does not entail a sequential set of enzymatic reactions that could be defined in terms of a pathway. Rather, various remodeling activities are required at different stages of signaling and repair. This seems to be generally reflected by the accumulation kinetics of core chromatin remodelers, with median t_{50} ranging from ∼17 to 50 s (Figure 4) and median t_{95} ∼55 to 220 s (Supplementary Figure S4). ALC1 and CHD2, known to interact with and stimulate the NHEJ machinery (57,59,136), accumulated with kinetics comparable to that of some NHEJ factors. In contrast, accumulation of SIRT7 and ACF1 was slower than of most NHEJ machinery, even though they have also been implicated in this pathway (65,137). CHD4 and SMARCA5, which assist in damage signaling, accumulated simultaneously with other signaling factors (32,37,60,138). In summary, our comprehensive and integrated analysis of published accumulation kinetics of DSBR proteins provides a general view on the temporal sequence of signaling, chromatin remodeling and repair events that occur at DSBs.

DISCUSSION

Our initial review of accumulation data (Figure 1) revealed a number of interesting observations. First, the vast majority of studies used HeLa or U2OS cells, even though other aspects of DSBR are commonly investigated in a broad range of normal and cancer cell lines. As a result, the behavior of repair proteins in normal cells, as well as

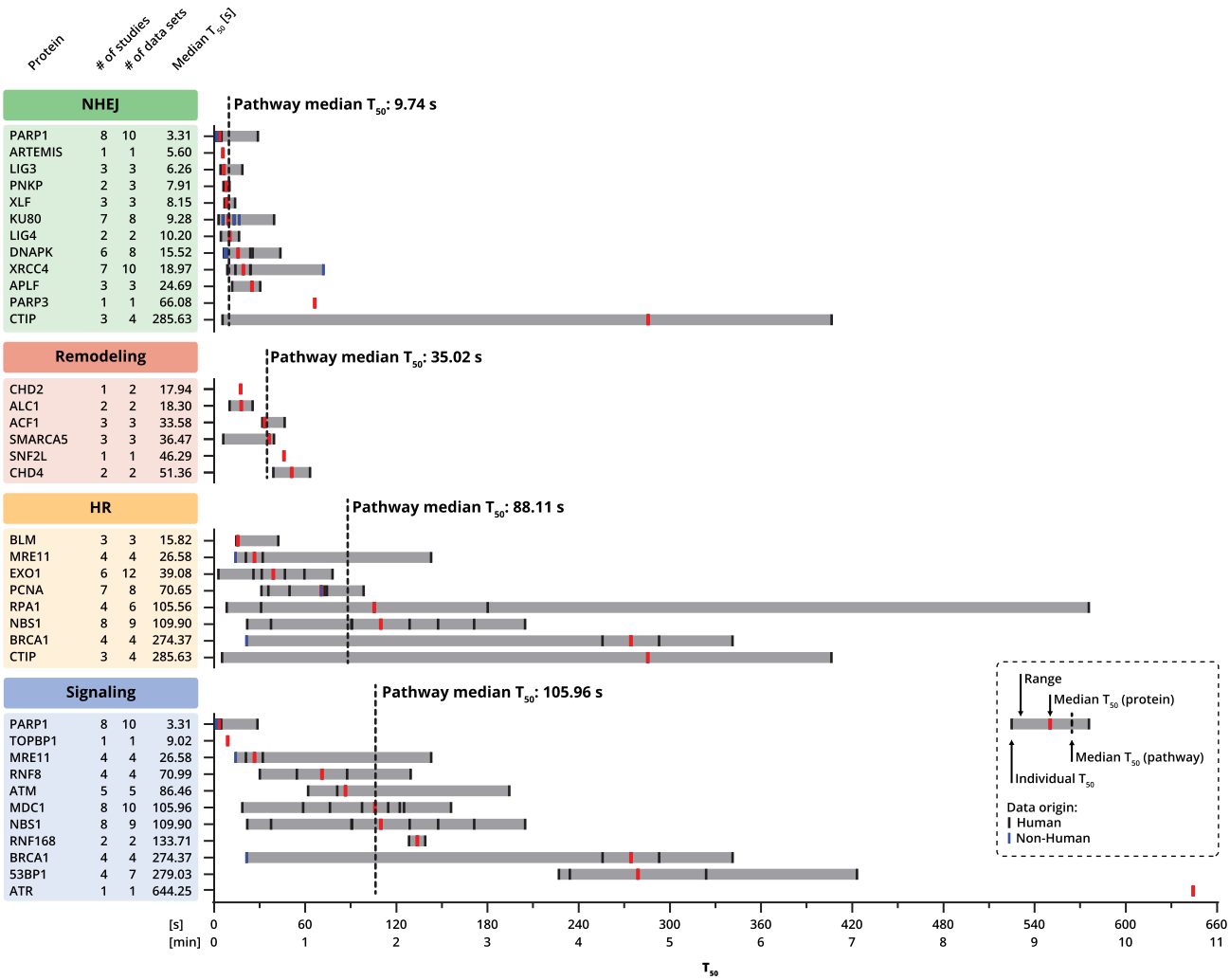

Figure 4. Proteins involved in different DSBR pathways are characterized by distinct accumulation kinetics. The core factors of each DSBR pathway were ordered by their accumulation t_{50}. Solid black and blue vertical lines indicate datasets originating from studies in human or non-human cells, respectively. Solid red vertical lines indicate the median t_{50} value for each protein. Dashed black vertical lines indicate the mean t_{50} of all proteins involved in the indicated pathway.

the differences between normal and cancer cells, remain practically unexplored. This is important, because differences in response of normal and cancer tissues to therapy-induced DNA damage might reveal novel treatment opportunities. Further, only a handful of studies (∼10%) investigated DSBR protein accumulation in mouse cells, even though numerous mutant or KO mouse models of DSBR factors are available. Second, the most commonly used technique for induction of DNA damage was laser microirradiation. More detailed analysis revealed, however, that the setup of these experiments, especially laser wavelength and sensitization method, varied considerably between studies, with few experiments performed using identical configurations. It is increasingly clear that different microirradiation and photosensitization methods produce different spectra and loads of DNA lesions (8,9,21,38,139,140), which can in turn affect the accumulation kinetics. This conclusion seems to be supported by our subsequent DSBR-wide analysis (Figure 3A). It is likely that the relatively large variability of reported accumulation speeds observed for many of DSBR proteins is at least in part a consequence of differences in experimental setup (e.g. cell line, presensitization method and laser wavelength or intensity). Unfortunately, based on our meta-analysis it is not feasible to pinpoint the exact source of this variability, as studies that reported data on a given DSBR protein usually differed in multiple aspects of experimental approach, and some important aspects (e.g. DSB load or the functionality of the fluorescently tagged proteins) were not reported. It should be noted that the measured accumulation is a derivative of the abundance of the protein in the cell nucleus relative to its enrichment at the damaged DNA/chromatin. This could be especially relevant when measuring accumulation of proteins that fulfill multiple repair functions which require different molecular concentrations. For instance, a protein that is required in low concentration in early phases of repair might be abundantly recruited in a later phase. Visualization of such proteins at sparsely damaged sites could fail

to reveal their involvement in early phases of repair and only reflect their late functions. Moreover, multiple proteins (e.g. PARP1, XRCC1, LIG3 or APLF) are involved in responses to DSBs as well as to other lesions that are likely induced by laser microirradiation. It is thus not feasible to determine whether the reported accumulation kinetics reflects their roles in DSBR or in other repair pathways. Our analysis thus strikes a cautionary note against direct comparisons of data from studies applying different methodology.

Detailed analysis of the accumulation of individual DSBR proteins (see Figure 3B and the online visualization tool accompanying this study) revealed that the accumulation generally followed first-order exponential kinetics. Even though one seminal study showed a better second-order fit for 53BP1 and MDC1 (18), data from other studies that analyzed these proteins were better described by the first-order equations. It could be speculated that the second-order fit, which describes a sigmoidal curve, would require careful monitoring of the early accumulation phase. This, however, may be impeded by the local bleaching of the fluorescent tag due to UV-laser microirradiation. Such bleaching was noticeable in only a handful of studies, which is surprising because most UV microirradiation techniques require a relatively intense laser pulse. The absence of bleaching could be explained if fluorescence intensities were normalized to the intensity measured immediately after damage induction, or if imaging started after the diffusion-driven recovery of fluorescence.

In the vast majority of cases, the accumulation was detected immediately after microirradiation. Among the notable exceptions was the accumulation of MDC1 and 53BP1 when damage was induced by accelerated heavy ions (21), in which case an accumulation delay, dependent on the applied radiation method, was clearly observed. It is not obvious whether this delay is specific to responses to complex damage, or whether it is simply masked in studies applying laser microirradiation (e.g. due to the previously described bleaching). In any case, it is apparent that (nearly) all components of the DSBR accumulate in unison, albeit with different speeds, which are reflected by the slope of the exponential accumulation curves (Supplementary Figure S3). Therefore, all components of repair machinery are locally available already in the first seconds or minutes after damage induction. Further, the assembly of most DSBR complexes seems fully accomplished after ∼15–20 min (Supplementary Figure S2). This is consistent with the notion that the DSBR is a generally fast process, with ∼50% of X-ray induced breaks reportedly cleared within 30–40 min (141).

Comparing accumulation of proteins involved in signaling, chromatin remodeling, NHEJ and HR (Figure 5), we found that NHEJ complexes are among the first to be assembled. This is in agreement with the model where DNA ends are bound by KU, which then either promotes recruitment of other NHEJ factors, with help of 53BP1 and REV1, or is evicted by CTIP/BRCA1, which promote HR (142,143). The accumulation of proteins involved in the latter pathway was indeed clearly slower. In line with the requirement for DNA resection prior to the assembly of HR machinery (144), MRE11, EXO1 and BLM were among the fastest of HR factors. Surprisingly, CTIP appeared to

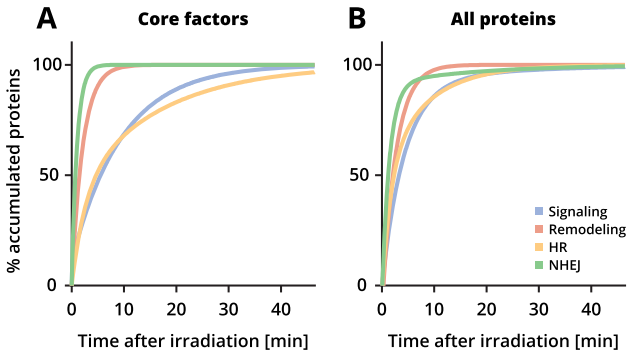

Figure 5. Schematic representation of DSBR kinetics. The curves represent the changes in the fraction of accumulated core factors (**A**) and all factors (**B**) involved in the indicated pathways, based on their t_{95} values.

be much slower, which is incompatible with its involvement in the repair pathway choice or in the early steps of HR, but one study did report very fast accumulation of this protein, comparable to some of NHEJ factors. Remarkably, the accumulation sequence of major signaling factors, derived from multiple independent studies, mirrored the generally accepted models (3). Assembly of complexes involved in chromatin remodeling spanned the entire temporal range of DSBR, which agrees with the multi-level, multi-functional and partly non-linear character of this process.

In conclusion, in spite of the relatively large inter-study variability of the published data, the results of our first comprehensive meta-analysis reveal some interesting insights. First, it appears that we know very little about the assembly kinetics of DSBR complexes in normal human cells or in response to clinically relevant DNA damage. Second, the accumulation of nearly 80 individual DSBR-related proteins starts immediately after damage induction, progresses in unison and is mostly completed within 15–20 min. Third, NHEJ factors are among the first to arrive at damage sites, followed by the slower HR machinery, while signaling and remodeling responses include fast, intermediate and slow components. These insights stress the complexity of mechanisms driving the mammalian DSBR and reveal the need for well-controlled, comprehensive studies in normal and cancer human cells.

AVAILABILITY

Openly accessible website accompanying this study is available at www.dna-repair.live/cumulus.

SUPPLEMENTARY DATA

Supplementary Data are available at NAR Online.

ACKNOWLEDGEMENTS

We thank Dr J.A. Aten for helpful discussions and Dr R.A. Hoebe for help with website hosting.

FUNDING

European Research Council Grants (ERC Consolidator) [617485 to H.v.A.]; Dutch Cancer Society (KWF

Kankerbestrijding) [EMCR 2015–7846 to P.M.K.]. Funding for open access charge: Dutch Cancer Society (KWF Kankerbestrijding) [EMCR 2015-7846].
Conflict of interest statement. None declared.

REFERENCES

1. Jackson,S.P. (2002) Sensing and repairing DNA double-strand breaks. *Carcinogenesis*, **23**, 687–696.
2. Polo,S.E. and Jackson,S.P. (2011) Dynamics of DNA damage response proteins at DNA breaks: a focus on protein modifications. *Genes Dev.*, **25**, 409–433.
3. Smeenk,G. and van Attikum,H. (2013) The chromatin response to DNA breaks: leaving a mark on genome integrity. *Annu. Rev. Biochem.*, **82**, 55–80.
4. Prakash,R., Zhang,Y., Feng,W. and Jasin,M. (2015) Homologous recombination and human health: the roles of BRCA1, BRCA2, and associated proteins. *Cold Spring Harb. Perspect. Biol.*, **7**, a016600.
5. Chang,H.H.Y., Pannunzio,N.R., Adachi,N. and Lieber,M.R. (2017) Non-homologous DNA end joining and alternative pathways to double-strand break repair. *Nat. Rev. Mol. Cell Biol.*, **18**, 495–506.
6. Lukas,C., Bartek,J. and Lukas,J. (2005) Imaging of protein movement induced by chromosomal breakage: tiny 'local' lesions pose great 'global' challenges. *Chromosoma*, **114**, 146–154.
7. Limoli,C.L. and Ward,J.F. (1993) A new method for introducing double-strand breaks into cellular DNA. *Radiat. Res.*, **134**, 160–169.
8. Dinant,C., de Jager,M., Essers,J., van Cappellen,W.A., Kanaar,R., Houtsmuller,A.B. and Vermeulen,W. (2007) Activation of multiple DNA repair pathways by sub-nuclear damage induction methods. *J. Cell Sci.*, **120**, 2731–2740.
9. Kong,X., Mohanty,S.K., Stephens,J., Heale,J.T., Gomez-Godinez,V., Shi,L.Z., Kim,J.-S., Yokomori,K. and Berns,M.W. (2009) Comparative analysis of different laser systems to study cellular responses to DNA damage in mammalian cells. *Nucleic Acids Res.*, **37**, e68.
10. Nelms,B.E., Maser,R.S., MacKay,J.F., Lagally,M.G. and Petrini,J.H. (1998) In situ visualization of DNA double-strand break repair in human fibroblasts. *Science*, **280**, 590–592.
11. van Oven,C., Krawczyk,P.M., Stap,J., Melo,A.M., Piazzetta,M.H.O., Gobbi,A.L., van Veen,H.A., Verhoeven,J. and Aten,J.A. (2009) An ultrasoft X-ray multi-microbeam irradiation system for studies of DNA damage responses by fixed- and live-cell fluorescence microscopy. *Eur. Biophys. J.*, **38**, 721–728.
12. Reynolds,P., Anderson,J.A., Harper,J.V., Hill,M.A., Botchway,S.W., Parker,A.W. and O'Neill,P. (2012) The dynamics of Ku70/80 and DNA-PKcs at DSBs induced by ionizing radiation is dependent on the complexity of damage. *Nucleic Acids Res.*, **40**, 10821–10831.
13. Aten,J.A., Stap,J., Krawczyk,P.M., van Oven,C.H., Hoebe,R.A., Essers,J. and Kanaar,R. (2004) Dynamics of DNA double-strand breaks revealed by clustering of damaged chromosome domains. *Science*, **303**, 92–95.
14. Jakob,B., Scholz,M. and Taucher-Scholz,G. (2002) Characterization of CDKN1A (p21) binding to sites of heavy-ion-induced damage: colocalization with proteins involved in DNA repair. *Int. J. Radiat. Biol.*, **78**, 75–88.
15. Jakob,B., Scholz,M. and Taucher-Scholz,G. (2003) Biological imaging of heavy charged-particle tracks. *Radiat. Res.*, **159**, 676–684.
16. Charlton,D., Nikjoo,H. and Humm,J. (1989) Calculation of initial yields of single- and double-strand breaks in cell nuclei from electrons, protons and alpha particles. *Int. J. Radiat. Biol.*, **56**, 1–19.
17. Goodhead,D.T. (1994) Initial events in the cellular effects of ionizing radiations: clustered damage in DNA. *Int. J. Radiat. Biol.*, **65**, 7–17.
18. Bekker-Jensen,S., Lukas,C., Melander,F., Bartek,J. and Lukas,J. (2005) Dynamic assembly and sustained retention of 53BP1 at the sites of DNA damage are controlled by Mdc1/NFBD1. *J. Cell Biol.*, **170**, 201–211.
19. Mailand,N., Bekker-Jensen,S., Faustrup,H., Melander,F., Bartek,J., Lukas,C. and Lukas,J. (2007) RNF8 ubiquitylates histones at DNA double-strand breaks and promotes assembly of repair proteins. *Cell*, **131**, 887–900.
20. Acs,K., Luijsterburg,M.S., Ackermann,L., Salomons,F.A., Hoppe,T. and Dantuma,N.P. (2011) The AAA-ATPase VCP/p97 promotes 53BP1 recruitment by removing L3MBTL1 from DNA double-strand breaks. *Nat. Struct. Mol. Biol.*, **18**, 1345–1350.
21. Hable,V., Drexler,G.A., Brüning,T., Burgdorf,C., Greubel,C., Derer,A., Seel,J., Strickfaden,H., Cremer,T., Friedl,A.A. *et al.* (2012) Recruitment kinetics of DNA repair proteins Mdc1 and Rad52 but not 53BP1 depend on damage complexity. *PLoS One*, **7**, e41943.
22. So,S., Davis,A.J. and Chen,D.J. (2009) Autophosphorylation at serine 1981 stabilizes ATM at DNA damage sites. *J. Cell Biol.*, **187**, 977–990.
23. Moyal,L., Lerenthal,Y., Gana-Weisz,M., Mass,G., So,S., Wang,S.-Y., Eppink,B., Chung,Y.M., Shalev,G., Shema,E. *et al.* (2011) Requirement of ATM-dependent monoubiquitylation of histone H2B for timely repair of DNA double-strand breaks. *Mol. Cell*, **41**, 529–542.
24. Tomimatsu,N., Mukherjee,B., Deland,K., Kurimasa,A., Bolderson,E., Khanna,K.K. and Burma,S. (2012) Exo1 plays a major role in DNA end resection in humans and influences double-strand break repair and damage signaling decisions. *DNA Repair*, **11**, 441–448.
25. Morris,C., Tomimatsu,N., Richard,D.J., Cluet,D., Burma,S., Khanna,K.K. and Jalinot,P. (2012) INT6/EIF3E interacts with ATM and is required for proper execution of the DNA damage response in human cells. *Cancer Res.*, **72**, 2006–2016.
26. Tobias,F., Löb,D., Lengert,N., Durante,M., Drossel,B., Taucher-Scholz,G. and Jakob,B. (2013) Spatiotemporal dynamics of early DNA damage response proteins on complex DNA lesions. *PLoS One*, **8**, e57953.
27. Yan,Q., Xu,R., Zhu,L., Cheng,X., Wang,Z., Manis,J. and Shipp,M.A. (2013) BAL1 and its partner E3 ligase, BBAP, link Poly(ADP-ribose) activation, ubiquitylation, and double-strand DNA repair independent of ATM, MDC1, and RNF8. *Mol. Cell. Biol.*, **33**, 845–857.
28. Ismail,I.H., Andrin,C., McDonald,D. and Hendzel,M.J. (2010) BMI1-mediated histone ubiquitylation promotes DNA double-strand break repair. *J. Cell Biol.*, **191**, 45–60.
29. Sustáčková,G., Kozubek,S., Stixová,L., Legartová,S., Matula,P., Orlova,D. and Bártová,E. (2012) Acetylation-dependent nuclear arrangement and recruitment of BMI1 protein to UV-damaged chromatin. *J. Cell. Physiol.*, **227**, 1838–1850.
30. Ismail,I.H., Gagné,J.-P., Caron,M.-C., McDonald,D., Xu,Z., Masson,J.-Y., Poirier,G.G. and Hendzel,M.J. (2012) CBX4-mediated SUMO modification regulates BMI1 recruitment at sites of DNA damage. *Nucleic Acids Res.*, **40**, 5497–5510.
31. Doil,C., Mailand,N., Bekker-Jensen,S., Menard,P., Larsen,D.H., Pepperkok,R., Ellenberg,J., Panier,S., Durocher,D., Bartek,J. *et al.* (2009) RNF168 binds and amplifies ubiquitin conjugates on damaged chromosomes to allow accumulation of repair proteins. *Cell*, **136**, 435–446.
32. Smeenk,G., Wiegant,W.W., Vrolijk,H., Solari,A.P., Pastink,A. and van Attikum,H. (2010) The NuRD chromatin–remodeling complex regulates signaling and repair of DNA damage. *J. Cell Biol.*, **190**, 741–749.
33. Gagné,J.-P., Pic,E., Isabelle,M., Krietsch,J., Ethier,C., Paquet,E., Kelly,I., Boutin,M., Moon,K.-M., Foster,L.J. *et al.* (2012) Quantitative proteomics profiling of the poly(ADP-ribose)-related response to genotoxic stress. *Nucleic Acids Res.*, **40**, 7788–7805.
34. Ha,K., Lee,G.E., Palii,S.S., Brown,K.D., Takeda,Y., Liu,K., Bhalla,K.N. and Robertson,K.D. (2011) Rapid and transient recruitment of DNMT1 to DNA double-strand breaks is mediated by its interaction with multiple components of the DNA damage response machinery. *Hum. Mol. Genet.*, **20**, 126–140.
35. Min,S., Jo,S., Lee,H.-S., Chae,S., Lee,J.-S., Ji,J.-H. and Cho,H. (2014) ATM-dependent chromatin remodeler Rsf-1 facilitates DNA damage checkpoints and homologous recombination repair. *Cell Cycle*, **13**, 666–677.
36. Lukas,C., Melander,F., Stucki,M., Falck,J., Bekker-Jensen,S., Goldberg,M., Lerenthal,Y., Jackson,S.P., Bartek,J. and Lukas,J. (2004) Mdc1 couples DNA double-strand break recognition by Nbs1 with its H2AX-dependent chromatin retention. *EMBO J.*, **23**, 2674–2683.
37. Smeenk,G., Wiegant,W.W., Marteijn,J.A., Luijsterburg,M.S., Sroczynski,N., Costelloe,T., Romeijn,R.J., Pastink,A., Mailand,N., Vermeulen,W. *et al.* (2013) Poly(ADP-ribosyl)ation links the

chromatin remodeler SMARCA5/SNF2H to RNF168-dependent DNA damage signaling. *J. Cell Sci.*, **126**, 889–903.
38. Haince,J.-F., McDonald,D., Rodrigue,A., Déry,U., Masson,J.-Y., Hendzel,M.J. and Poirier,G.G. (2008) PARP1-dependent kinetics of recruitment of MRE11 and NBS1 proteins to multiple DNA damage sites. *J. Biol. Chem.*, **283**, 1197–1208.
39. Lu,C.-S., Truong,L.N., Aslanian,A., Shi,L.Z., Li,Y., Hwang,P.Y.-H., Koh,K.H., Hunter,T., Yates,J.R. 3rd, Berns,M.W. *et al.* (2012) The RING finger protein RNF8 ubiquitinates Nbs1 to promote DNA double-strand break repair by homologous recombination. *J. Biol. Chem.*, **287**, 43984–43994.
40. Lan,L., Nakajima,S., Komatsu,K., Nussenzweig,A., Shimamoto,A., Oshima,J. and Yasui,A. (2005) Accumulation of Werner protein at DNA double-strand breaks in human cells. *J. Cell Sci.*, **118**, 4153–4162.
41. Larsen,D.H., Hari,F., Clapperton,J.A., Gwerder,M., Gutsche,K., Altmeyer,M., Jungmichel,S., Toledo,L.I., Fink,D., Rask,M.-B. *et al.* (2014) The NBS1-Treacle complex controls ribosomal RNA transcription in response to DNA damage. *Nat. Cell Biol.*, **16**, 792–803.
42. Ha,K., Takeda,Y. and Dynan,W.S. (2011) Sequences in PSF/SFPQ mediate radioresistance and recruitment of PSF/SFPQ-containing complexes to DNA damage sites in human cells. *DNA Repair*, **10**, 252–259.
43. Kuhnert,A., Schmidt,U., Monajembashi,S., Franke,C., Schlott,B., Grosse,F., Greulich,K.O., Saluz,H.-P. and Hänel,F. (2012) Proteomic identification of PSF and p54(nrb) as TopBP1-interacting proteins. *J. Cell. Biochem.*, **113**, 1744–1753.
44. Krietsch,J., Caron,M.-C., Gagné,J.-P., Ethier,C., Vignard,J., Vincent,M., Rouleau,M., Hendzel,M.J., Poirier,G.G. and Masson,J.-Y. (2012) PARP activation regulates the RNA-binding protein NONO in the DNA damage response to DNA double-strand breaks. *Nucleic Acids Res.*, **40**, 10287–10301.
45. Kobayashi,J., Fujimoto,H., Sato,J., Hayashi,I., Burma,S., Matsuura,S., Chen,D.J. and Komatsu,K. (2012) Nucleolin participates in DNA double-strand break-induced damage response through MDC1-dependent pathway. *PLoS One*, **7**, e49245.
46. Boudra,M.-T., Bolin,C., Chiker,S., Fouquin,A., Zaremba,T., Vaslin,L., Biard,D., Cordelières,F.P., Mégnin-Chanet,F., Favaudon,V. *et al.* (2015) PARP-2 depletion results in lower radiation cell survival but cell line-specific differences in poly(ADP-ribose) levels. *Cell. Mol. Life Sci.*, **72**, 1585–1597.
47. Hong,Z., Jiang,J., Ma,J., Dai,S., Xu,T., Li,H. and Yasui,A. (2013) The role of hnRPUL1 involved in DNA damage response is related to PARP1. *PLoS One*, **8**, e60208.
48. Abdou,I., Poirier,G.G., Hendzel,M.J. and Weinfeld,M. (2015) DNA ligase III acts as a DNA strand break sensor in the cellular orchestration of DNA strand break repair. *Nucleic Acids Res.*, **43**, 875–892.
49. Young,L.M., Marzio,A., Perez-Duran,P., Reid,D.A., Meredith,D.N., Roberti,D., Star,A., Rothenberg,E., Ueberheide,B. and Pagano,M. (2015) TIMELESS forms a complex with PARP1 distinct from its complex with TIPIN and plays a role in the DNA damage response. *Cell Rep.*, **13**, 451–459.
50. Nakajima,S., Lan,L., Kanno,S.-I., Usami,N., Kobayashi,K., Mori,M., Shiomi,T. and Yasui,A. (2006) Replication-dependent and -independent responses of RAD18 to DNA damage in human cells. *J. Biol. Chem.*, **281**, 34687–34695.
51. Kang,H.C., Lee,Y.-I., Shin,J.-H., Andrabi,S.A., Chi,Z., Gagné,J.-P., Lee,Y., Ko,H.S., Lee,B.D., Poirier,G.G. *et al.* (2011) Iduna is a poly(ADP-ribose) (PAR)-dependent E3 ubiquitin ligase that regulates DNA damage. *Proc. Natl. Acad. Sci. U.S.A.*, **108**, 14103–14108.
52. Shima,H., Suzuki,H., Sun,J., Kono,K., Shi,L., Kinomura,A., Horikoshi,Y., Ikura,T., Ikura,M., Kanaar,R. *et al.* (2013) Activation of the SUMO modification system is required for the accumulation of RAD51 at sites of DNA damage. *J. Cell Sci.*, **126**, 5284–5292.
53. Xie,S., Mortusewicz,O., Ma,H.T., Herr,P., Poon,R.Y.C., Poon,R.R.Y., Helleday,T. and Qian,C. (2015) Timeless interacts with PARP-1 to promote homologous recombination repair. *Mol. Cell*, **60**, 163–176.
54. Erdel,F. and Rippe,K. (2011) Binding kinetics of human ISWI chromatin-remodelers to DNA repair sites elucidate their target location mechanism. *Nucleus*, **2**, 105–112.
55. Sánchez-Molina,S., Mortusewicz,O., Bieber,B., Auer,S., Eckey,M., Leonhardt,H., Friedl,A.A. and Becker,P.B. (2011) Role for hACF1 in the G2/M damage checkpoint. *Nucleic Acids Res.*, **39**, 8445–8456.
56. Klement,K., Luijsterburg,M.S., Pinder,J.B., Cena,C.S., Del Nero,V., Wintersinger,C.M., Dellaire,G., van Attikum,H. and Goodarzi,A.A. (2014) Opposing ISWI- and CHD-class chromatin remodeling activities orchestrate heterochromatic DNA repair. *J. Cell Biol.*, **207**, 717–733.
57. Ahel,D., Horejsí,Z., Wiechens,N., Polo,S.E., Garcia-Wilson,E., Ahel,I., Flynn,H., Skehel,M., West,S.C., Jackson,S.P. *et al.* (2009) Poly(ADP-ribose)-dependent regulation of DNA repair by the chromatin remodeling enzyme ALC1. *Science*, **325**, 1240–1243.
58. Pines,A., Vrouwe,M.G., Marteijn,J.A., Typas,D., Luijsterburg,M.S., Cansoy,M., Hensbergen,P., Deelder,A., de Groot,A., Matsumoto,S. *et al.* (2012) PARP1 promotes nucleotide excision repair through DDB2 stabilization and recruitment of ALC1. *J. Cell Biol.*, **199**, 235–249.
59. Luijsterburg,M.S., de Krijger,I., Wiegant,W.W., Shah,R.G., Smeenk,G., de Groot,A.J.L., Pines,A., Vertegaal,A.C.O., Jacobs,J.J.L., Shah,G.M. *et al.* (2016) PARP1 links CHD2-mediated chromatin expansion and H3.3 deposition to DNA repair by non-homologous end-joining. *Mol. Cell*, **61**, 547–562.
60. Larsen,D.H., Poinsignon,C., Gudjonsson,T., Dinant,C., Payne,M.R., Hari,F.J., Rendtlew Danielsen,J.M., Menard,P., Sand,J.C., Stucki,M. *et al.* (2010) The chromatin-remodeling factor CHD4 coordinates signaling and repair after DNA damage. *J. Cell Biol.*, **190**, 731–740.
61. Campbell,S., Ismail,I.H., Young,L.C., Poirier,G.G. and Hendzel,M.J. (2013) Polycomb repressive complex 2 contributes to DNA double-strand break repair. *Cell Cycle*, **12**, 2675–2683.
62. Young,L.C., McDonald,D.W. and Hendzel,M.J. (2013) Kdm4b histone demethylase is a DNA damage response protein and confers a survival advantage following γ-irradiation. *J. Biol. Chem.*, **288**, 21376–21388.
63. Khoury-Haddad,H., Guttmann-Raviv,N., Ipenberg,I., Huggins,D., Jeyasekharan,A.D. and Ayoub,N. (2014) PARP1-dependent recruitment of KDM4D histone demethylase to DNA damage sites promotes double-strand break repair. *Proc. Natl. Acad. Sci. U.S.A.*, **111**, E728–E737.
64. Alatwi,H.E. and Downs,J.A. (2015) Removal of H2A.Z by INO80 promotes homologous recombination. *EMBO Rep.*, **16**, 986–994.
65. Vazquez,B.N., Thackray,J.K., Simonet,N.G., Kane-Goldsmith,N., Martinez-Redondo,P., Nguyen,T., Bunting,S., Vaquero,A., Tischfield,J.A. and Serrano,L. (2016) SIRT7 promotes genome integrity and modulates non-homologous end joining DNA repair. *EMBO J.*, **35**, 1488–1503.
66. Li,L., Shi,L., Yang,S., Yan,R., Zhang,D., Yang,J., He,L., Li,W., Yi,X., Sun,L. *et al.* (2016) SIRT7 is a histone desuccinylase that functionally links to chromatin compaction and genome stability. *Nat. Commun.*, **7**, 12235.
67. Aydin,Ö.Z., Marteijn,J.A., Ribeiro-Silva,C., Rodríguez López,A., Wijgers,N., Smeenk,G., van Attikum,H., Poot,R.A., Vermeulen,W. and Lans,H. (2014) Human ISWI complexes are targeted by SMARCA5 ATPase and SLIDE domains to help resolve lesion-stalled transcription. *Nucleic Acids Res.*, **42**, 8473–8485.
68. Fujita,K., Nakamura,Y., Oka,T., Ito,H., Tamura,T., Tagawa,K., Sasabe,T., Katsuta,A., Motoki,K., Shiwaku,H. *et al.* (2013) A functional deficiency of TERA/VCP/p97 contributes to impaired DNA repair in multiple polyglutamine diseases. *Nat. Commun.*, **4**, 1816.
69. Singh,D.K., Karmakar,P., Aamann,M., Schurman,S.H., May,A., Croteau,D.L., Burks,L., Plon,S.E. and Bohr,V.A. (2010) The involvement of human RECQL4 in DNA double-strand break repair. *Aging Cell*, **9**, 358–371.
70. Popuri,V., Ramamoorthy,M., Tadokoro,T., Singh,D.K., Karmakar,P., Croteau,D.L. and Bohr,V.A. (2012) Recruitment and retention dynamics of RECQL5 at DNA double strand break sites. *DNA Repair*, **11**, 624–635.
71. Khadka,P., Hsu,J.K., Veith,S., Tadokoro,T., Shamanna,R.A., Mangerich,A., Croteau,D.L. and Bohr,V.A. (2015) Differential and concordant roles for Poly(ADP-Ribose) polymerase 1 and Poly(ADP-Ribose) in regulating WRN and RECQL5 activities. *Mol. Cell. Biol.*, **35**, 3974–3989.

72. Ismail,I.H., Davidson,R., Gagné,J.-P., Xu,Z.Z., Poirier,G.G. and Hendzel,M.J. (2014) Germline mutations in BAP1 impair its function in DNA double-strand break repair. *Cancer Res.*, **74**, 4282–4294.
73. Lu,H., Shamanna,R.A., Keijzers,G., Anand,R., Rasmussen,L.J., Cejka,P., Croteau,D.L. and Bohr,V.A. (2016) RECQL4 promotes DNA end resection in repair of DNA double-strand breaks. *Cell Rep.*, **16**, 161–173.
74. Qvist,P., Huertas,P., Jimeno,S., Nyegaard,M., Hassan,M.J., Jackson,S.P. and Børglum,A.D. (2011) CtIP mutations cause Seckel and Jawad syndromes. *PLoS Genet.*, **7**, e1002310.
75. Wang,H., Shao,Z., Shi,L.Z., Hwang,P.Y.-H., Truong,L.N., Berns,M.W., Chen,D.J. and Wu,X. (2012) CtIP protein dimerization is critical for its recruitment to chromosomal DNA double-stranded breaks. *J. Biol. Chem.*, **287**, 21471–21480.
76. Bolderson,E., Tomimatsu,N., Richard,D.J., Boucher,D., Kumar,R., Pandita,T.K., Burma,S. and Khanna,K.K. (2010) Phosphorylation of Exo1 modulates homologous recombination repair of DNA double-strand breaks. *Nucleic Acids Res.*, **38**, 1821–1831.
77. Chen,X., Paudyal,S.C., Chin,R.-I. and You,Z. (2013) PCNA promotes processive DNA end resection by Exo1. *Nucleic Acids Res.*, **41**, 9325–9338.
78. Nishi,R., Wijnhoven,P., le Sage,C., Tjeertes,J., Galanty,Y., Forment,J.V., Clague,M.J., Urbé,S. and Jackson,S.P. (2014) Systematic characterization of deubiquitylating enzymes for roles in maintaining genome integrity. *Nat. Cell Biol.*, **16**, 1016–1026.
79. Chen,X., Kim,I.-K., Honaker,Y., Paudyal,S.C., Koh,W.K., Sparks,M., Li,S., Piwnica-Worms,H., Ellenberger,T. and You,Z. (2015) 14-3-3 proteins restrain the Exo1 nuclease to prevent overresection. *J. Biol. Chem.*, **290**, 12300–12312.
80. Cheruiyot,A., Paudyal,S.C., Kim,I.-K., Sparks,M., Ellenberger,T., Piwnica-Worms,H. and You,Z. (2015) Poly(ADP-ribose)-binding promotes Exo1 damage recruitment and suppresses its nuclease activities. *DNA Repair*, **35**, 106–115.
81. Sherry,M.R., Hay,T.J.M., Gulak,M.A., Nassiri,A., Finnen,R.L. and Banfield,B.W. (2017) The Herpesvirus nuclear egress complex component, UL31, can be recruited to sites of DNA damage through Poly-ADP ribose binding. *Sci. Rep.*, **7**, 1882.
82. Hashiguchi,K., Matsumoto,Y. and Yasui,A. (2007) Recruitment of DNA repair synthesis machinery to sites of DNA damage/repair in living human cells. *Nucleic Acids Res.*, **35**, 2913–2923.
83. Godon,C., Cordelières,F.P., Biard,D., Giocanti,N., Mégnin-Chanet,F., Hall,J. and Favaudon,V. (2008) PARP inhibition versus PARP-1 silencing: different outcomes in terms of single-strand break repair and radiation susceptibility. *Nucleic Acids Res.*, **36**, 4454–4464.
84. Mortusewicz,O., Fouquerel,E., Amé,J.-C., Leonhardt,H. and Schreiber,V. (2011) PARG is recruited to DNA damage sites through poly(ADP-ribose)- and PCNA-dependent mechanisms. *Nucleic Acids Res.*, **39**, 5045–5056.
85. Wiese,C., Rudolph,J.H., Jakob,B., Fink,D., Tobias,F., Blattner,C. and Taucher-Scholz,G. (2012) PCNA-dependent accumulation of CDKN1A into nuclear foci after ionizing irradiation. *DNA Repair*, **11**, 511–521.
86. Khurana,S., Kruhlak,M.J., Kim,J., Tran,A.D., Liu,J., Nyswaner,K., Shi,L., Jailwala,P., Sung,M.-H., Hakim,O. *et al.* (2014) A macrohistone variant links dynamic chromatin compaction to BRCA1-dependent genome maintenance. *Cell Rep.*, **8**, 1049–1062.
87. Sharma,V., Khurana,S., Kubben,N., Abdelmohsen,K., Oberdoerffer,P., Gorospe,M. and Misteli,T. (2015) A BRCA1-interacting lncRNA regulates homologous recombination. *EMBO Rep.*, **16**, 1520–1534.
88. Soo Lee,N., Jin Chung,H., Kim,H.-J., Yun Lee,S., Ji,J.-H., Seo,Y., Hun Han,S., Choi,M., Yun,M., Lee,S.-G. *et al.* (2016) TRAIP/RNF206 is required for recruitment of RAP80 to sites of DNA damage. *Nat. Commun.*, **7**, 10463.
89. Ismail,I.H., Gagné,J.-P., Genois,M.-M., Strickfaden,H., McDonald,D., Xu,Z., Poirier,G.G., Masson,J.-Y. and Hendzel,M.J. (2015) The RNF138 E3 ligase displaces Ku to promote DNA end resection and regulate DNA repair pathway choice. *Nat. Cell Biol.*, **17**, 1446–1457.
90. Marteijn,J.A., Bekker-Jensen,S., Mailand,N., Lans,H., Schwertman,P., Gourdin,A.M., Dantuma,N.P., Lukas,J. and Vermeulen,W. (2009) Nucleotide excision repair-induced H2A ubiquitination is dependent on MDC1 and RNF8 and reveals a universal DNA damage response. *J. Cell Biol.*, **186**, 835–847.
91. Barclay,S.S., Tamura,T., Ito,H., Fujita,K., Tagawa,K., Shimamura,T., Katsuta,A., Shiwaku,H., Sone,M., Imoto,S. *et al.* (2014) Systems biology analysis of Drosophila in vivo screen data elucidates core networks for DNA damage repair in SCA1. *Hum. Mol. Genet.*, **23**, 1345–1364.
92. Gilmore,J.M., Sardiu,M.E., Groppe,B.D., Thornton,J.L., Liu,X., Dayebgadoh,G., Banks,C.A., Slaughter,B.D., Unruh,J.R., Workman,J.L. *et al.* (2016) WDR76 Co-localizes with heterochromatin related proteins and rapidly responds to DNA damage. *PLoS One*, **11**, e0155492.
93. Demuth,I., Bradshaw,P.S., Lindner,A., Anders,M., Heinrich,S., Kallenbach,J., Schmelz,K., Digweed,M., Meyn,M.S. and Concannon,P. (2008) Endogenous hSNM1B/Apollo interacts with TRF2 and stimulates ATM in response to ionizing radiation. *DNA Repair*, **7**, 1192–1201.
94. Tanikawa,M., Sanjiv,K., Helleday,T., Herr,P. and Mortusewicz,O. (2016) The spliceosome U2 snRNP factors promote genome stability through distinct mechanisms; transcription of repair factors and R-loop processing. *Oncogenesis*, **5**, e280.
95. Leung,J.W.C., Makharashvili,N., Agarwal,P., Chiu,L.-Y., Pourpre,R., Cammarata,M.B., Cannon,J.R., Sherker,A., Durocher,D., Brodbelt,J.S. *et al.* (2017) ZMYM3 regulates BRCA1 localization at damaged chromatin to promote DNA repair. *Genes Dev.*, **31**, 260–274.
96. Li,G.-Y., McCulloch,R.D., Fenton,A.L., Cheung,M., Meng,L., Ikura,M. and Koch,C.A. (2010) Structure and identification of ADP-ribose recognition motifs of APLF and role in the DNA damage response. *Proc. Natl. Acad. Sci. U.S.A.*, **107**, 9129–9134.
97. Grundy,G.J., Rulten,S.L., Zeng,Z., Arribas-Bosacoma,R., Iles,N., Manley,K., Oliver,A. and Caldecott,K.W. (2013) APLF promotes the assembly and activity of non-homologous end joining protein complexes. *EMBO J.*, **32**, 112–125.
98. Fenton,A.L., Shirodkar,P., Macrae,C.J., Meng,L. and Koch,C.A. (2013) The PARP3- and ATM-dependent phosphorylation of APLF facilitates DNA double-strand break repair. *Nucleic Acids Res.*, **41**, 4080–4092.
99. Uematsu,N., Weterings,E., Yano,K.-I., Morotomi-Yano,K., Jakob,B., Taucher-Scholz,G., Mari,P.-O., van Gent,D.C., Chen,B.P.C. and Chen,D.J. (2007) Autophosphorylation of DNA-PKCS regulates its dynamics at DNA double-strand breaks. *J. Cell Biol.*, **177**, 219–229.
100. Li,A.Y.J., Boo,L.M., Wang,S.-Y., Lin,H.H., Wang,C.C.C., Yen,Y., Chen,B.P.C., Chen,D.J. and Ann,D.K. (2009) Suppression of nonhomologous end joining repair by overexpression of HMGA2. *Cancer Res.*, **69**, 5699–5706.
101. Sharma,G.G., So,S., Gupta,A., Kumar,R., Cayrou,C., Avvakumov,N., Bhadra,U., Pandita,R.K., Porteus,M.H., Chen,D.J. *et al.* (2010) MOF and histone H4 acetylation at lysine 16 are critical for DNA damage response and double-strand break repair. *Mol. Cell. Biol.*, **30**, 3582–3595.
102. Davis,A.J., So,S. and Chen,D.J. (2010) Dynamics of the PI3K-like protein kinase members ATM and DNA-PKcs at DNA double strand breaks. *Cell Cycle*, **9**, 2529–2536.
103. Toulany,M., Lee,K.-J., Fattah,K.R., Lin,Y.-F., Fehrenbacher,B., Schaller,M., Chen,B.P., Chen,D.J. and Rodemann,H.P. (2012) Akt promotes post-irradiation survival of human tumor cells through initiation, progression, and termination of DNA-PKcs-dependent DNA double-strand break repair. *Mol. Cancer Res.*, **10**, 945–957.
104. Mori,E., Davis,A.J., Hasegawa,M. and Chen,D.J. (2016) Lysines 3241 and 3260 of DNA-PKcs are important for genomic stability and radioresistance. *Biochem. Biophys. Res. Commun.*, **477**, 235–240.
105. Mari,P.-O., Florea,B.I., Persengiev,S.P., Verkaik,N.S., Brüggenwirth,H.T., Modesti,M., Giglia-Mari,G., Bezstarosti,K., Demmers,J.A.A., Luider,T.M. *et al.* (2006) Dynamic assembly of end-joining complexes requires interaction between Ku70/80 and XRCC4. *Proc. Natl. Acad. Sci. U.S.A.*, **103**, 18597–18602.
106. Wei,L., Lan,L., Hong,Z., Yasui,A., Ishioka,C. and Chiba,N. (2008) Rapid recruitment of BRCA1 to DNA double-strand breaks is dependent on its association with Ku80. *Mol. Cell. Biol.*, **28**, 7380–7393.
107. Andrin,C., McDonald,D., Attwood,K.M., Rodrigue,A., Ghosh,S., Mirzayans,R., Masson,J.-Y., Dellaire,G. and Hendzel,M.J. (2012) A

requirement for polymerized actin in DNA double-strand break repair. *Nucleus*, **3**, 384–395.
108. Grundy,G.J., Rulten,S.L., Arribas-Bosacoma,R., Davidson,K., Kozik,Z., Oliver,A.W., Pearl,L.H. and Caldecott,K.W. (2016) The Ku-binding motif is a conserved module for recruitment and stimulation of non-homologous end-joining proteins. *Nat. Commun.*, **7**, 11242.
109. Mortusewicz,O., Rothbauer,U., Cardoso,M.C. and Leonhardt,H. (2006) Differential recruitment of DNA Ligase I and III to DNA repair sites. *Nucleic Acids Res.*, **34**, 3523–3532.
110. Berg,E., Christensen,M.O., Dalla Rosa,I., Wannagat,E., Jänicke,R.U., Rösner,L.M., Dirks,W.G., Boege,F. and Mielke,C. (2011) XRCC4 controls nuclear import and distribution of Ligase IV and exchanges faster at damaged DNA in complex with Ligase IV. *DNA Repair*, **10**, 1232–1242.
111. Liu,X.-S., Chandramouly,G., Rass,E., Guan,Y., Wang,G., Hobbs,R.M., Rajendran,A., Xie,A., Shah,J.V., Davis,A.J. *et al.* (2015) LRF maintains genome integrity by regulating the non-homologous end joining pathway of DNA repair. *Nat. Commun.*, **6**, 8325.
112. Kaufmann,T., Grishkovskaya,I., Polyansky,A.A., Kostrhon,S., Kukolj,E., Olek,K.M., Herbert,S., Beltzung,E., Mechtler,K., Peterbauer,T. *et al.* (2017) A novel non-canonical PIP-box mediates PARG interaction with PCNA. *Nucleic Acids Res.*, **45**, 9741–9759.
113. Mortusewicz,O., Amé,J.-C., Schreiber,V. and Leonhardt,H. (2007) Feedback-regulated poly(ADP-ribosyl)ation by PARP-1 is required for rapid response to DNA damage in living cells. *Nucleic Acids Res.*, **35**, 7665–7675.
114. Grundy,G.J., Polo,L.M., Zeng,Z., Rulten,S.L., Hoch,N.C., Paomephan,P., Xu,Y., Sweet,S.M., Thorne,A.W., Oliver,A.W. *et al.* (2016) PARP3 is a sensor of nicked nucleosomes and monoribosylates histone H2B(Glu2). *Nat. Commun.*, **7**, 12404.
115. Musselman,C.A., Avvakumov,N., Watanabe,R., Abraham,C.G., Lalonde,M.-E., Hong,Z., Allen,C., Roy,S., Nuñez,J.K., Nickoloff,J. *et al.* (2012) Molecular basis for H3K36me3 recognition by the Tudor domain of PHF1. *Nat. Struct. Mol. Biol.*, **19**, 1266–1272.
116. Zolner,A.E., Abdou,I., Ye,R., Mani,R.S., Fanta,M., Yu,Y., Douglas,P., Tahbaz,N., Fang,S., Dobbs,T. *et al.* (2011) Phosphorylation of polynucleotide kinase/ phosphatase by DNA-dependent protein kinase and ataxia-telangiectasia mutated regulates its association with sites of DNA damage. *Nucleic Acids Res.*, **39**, 9224–9237.
117. Yano,K.-I., Morotomi-Yano,K., Wang,S.-Y., Uematsu,N., Lee,K.-J., Asaithamby,A., Weterings,E. and Chen,D.J. (2008) Ku recruits XLF to DNA double-strand breaks. *EMBO Rep.*, **9**, 91–96.
118. Hanssen-Bauer,A., Solvang-Garten,K., Gilljam,K.M., Torseth,K., Wilson,D.M. 3rd, Akbari,M. and Otterlei,M. (2012) The region of XRCC1 which harbours the three most common nonsynonymous polymorphic variants, is essential for the scaffolding function of XRCC1. *DNA Repair*, **11**, 357–366.
119. Tadokoro,T., Ramamoorthy,M., Popuri,V., May,A., Tian,J., Sykora,P., Rybanska,I., Wilson,D.M. 3rd, Croteau,D.L. and Bohr,V.A. (2012) Human RECQL5 participates in the removal of endogenous DNA damage. *Mol. Biol. Cell*, **23**, 4273–4285.
120. Campalans,A., Kortulewski,T., Amouroux,R., Menoni,H., Vermeulen,W. and Radicella,J.P. (2013) Distinct spatiotemporal patterns and PARP dependence of XRCC1 recruitment to single-strand break and base excision repair. *Nucleic Acids Res.*, **41**, 3115–3129.
121. Breslin,C., Hornyak,P., Ridley,A., Rulten,S.L., Hanzlikova,H., Oliver,A.W. and Caldecott,K.W. (2015) The XRCC1 phosphate-binding pocket binds poly (ADP-ribose) and is required for XRCC1 function. *Nucleic Acids Res.*, **43**, 6934–6944.
122. Iyama,T. and Wilson,D.M. 3rd (2016) Elements that regulate the DNA damage response of proteins defective in Cockayne syndrome. *J. Mol. Biol.*, **428**, 62–78.
123. Guo,N., Du,G., Liu,W., Guo,J., Wu,R., Chen,H. and Wei,J. (2016) Live cell imaging combined with high-energy single-ion microbeam. *Rev. Sci. Instrum.*, **87**, 034301.
124. Yano,K.-I. and Chen,D.J. (2008) Live cell imaging of XLF and XRCC4 reveals a novel view of protein assembly in the non-homologous end-joining pathway. *Cell Cycle*, **7**, 1321–1325.
125. Rulten,S.L., Fisher,A.E.O., Robert,I., Zuma,M.C., Rouleau,M., Ju,L., Poirier,G., Reina-San-Martin,B. and Caldecott,K.W. (2011) PARP-3 and APLF function together to accelerate nonhomologous end-joining. *Mol. Cell*, **41**, 33–45.
126. Deriano,L. and Roth,D.B. (2013) Modernizing the nonhomologous end-joining repertoire: alternative and classical NHEJ share the stage. *Annu. Rev. Genet.*, **47**, 433–455.
127. Jasin,M. and Rothstein,R. (2013) Repair of strand breaks by homologous recombination. *Cold Spring Harb. Perspect. Biol.*, **5**, a012740.
128. Hustedt,N. and Durocher,D. (2016) The control of DNA repair by the cell cycle. *Nat. Cell Biol.*, **19**, 1–9.
129. Kolas,N.K., Chapman,J.R., Nakada,S., Ylanko,J., Chahwan,R., Sweeney,F.D., Panier,S., Mendez,M., Wildenhain,J., Thomson,T.M. *et al.* (2007) Orchestration of the DNA-damage response by the RNF8 ubiquitin ligase. *Science*, **318**, 1637–1640.
130. Radhakrishnan,S.K., Jette,N. and Lees-Miller,S.P. (2014) Non-homologous end joining: emerging themes and unanswered questions. *DNA Repair*, **17**, 2–8.
131. Strande,N., Roberts,S.A., Oh,S., Hendrickson,E.A. and Ramsden,D.A. (2012) Specificity of the dRP/AP lyase of Ku promotes nonhomologous end joining (NHEJ) fidelity at damaged ends. *J. Biol. Chem.*, **287**, 13686–13693.
132. Roberts,S.A., Strande,N., Burkhalter,M.D., Strom,C., Havener,J.M., Hasty,P. and Ramsden,D.A. (2010) Ku is a 5'-dRP/AP lyase that excises nucleotide damage near broken ends. *Nature*, **464**, 1214–1217.
133. Ochi,T., Blackford,A.N., Coates,J., Jhujh,S., Mehmood,S., Tamura,N., Travers,J., Wu,Q., Draviam,V.M., Robinson,C.V. *et al.* (2015) PAXX, a paralog of XRCC4 and XLF, interacts with Ku to promote DNA double-strand break repair. *Science*, **347**, 185–188.
134. Dueva,R. and Iliakis,G. (2013) Alternative pathways of non-homologous end joining (NHEJ) in genomic instability and cancer. *Transl. Cancer Res.*, **2**, 163–177.
135. Symington,L.S. and Gautier,J. (2011) Double-strand break end resection and repair pathway choice. *Annu. Rev. Genet.*, **45**, 247–271.
136. Pines,A., Mullenders,L.H., van Attikum,H. and Luijsterburg,M.S. (2013) Touching base with PARPs: moonlighting in the repair of UV lesions and double-strand breaks. *Trends Biochem. Sci.*, **38**, 321–330.
137. Lan,L., Ui,A., Nakajima,S., Hatakeyama,K., Hoshi,M., Watanabe,R., Janicki,S.M., Ogiwara,H., Kohno,T., Kanno,S.-I. *et al.* (2010) The ACF1 complex is required for DNA double-strand break repair in human cells. *Mol. Cell*, **40**, 976–987.
138. Polo,S.E., Kaidi,A., Baskcomb,L., Galanty,Y. and Jackson,S.P. (2010) Regulation of DNA-damage responses and cell-cycle progression by the chromatin remodelling factor CHD4. *EMBO J.*, **29**, 3130–3139.
139. Gassman,N.R. and Wilson,S.H. (2015) Micro-irradiation tools to visualize base excision repair and single-strand break repair. *DNA Repair*, **31**, 52–63.
140. Muster,B., Rapp,A. and Cardoso,C.M. (2017) Systematic analysis of DNA damage induction and DNA repair pathway activation by continuous wave visible light laser micro-irradiation. *AIMS Genet.*, **4**, 47–68.
141. Bradley,M.O. and Kohn,K.W. (1979) X-ray induced DNA double strand break production and repair in mammalian cells as measured by neutral filter elution. *Nucleic Acids Res.*, **7**, 793–804.
142. Escribano-Díaz,C., Orthwein,A., Fradet-Turcotte,A., Xing,M., Young,J.T.F., Tkáč,J., Cook,M.A., Rosebrock,A.P., Munro,M., Canny,M.D. *et al.* (2013) A cell cycle-dependent regulatory circuit composed of 53BP1-RIF1 and BRCA1-CtIP controls DNA repair pathway choice. *Mol. Cell*, **49**, 872–883.
143. Chapman,J.R., Barral,P., Vannier,J.-B., Borel,V., Steger,M., Tomas-Loba,A., Sartori,A.A., Adams,I.R., Batista,F.D. and Boulton,S.J. (2013) RIF1 is essential for 53BP1-dependent nonhomologous end joining and suppression of DNA double-strand break resection. *Mol. Cell*, **49**, 858–871.
144. Symington,L.S. (2016) Mechanism and regulation of DNA end resection in eukaryotes. *Crit. Rev. Biochem. Mol. Biol.*, **51**, 195–212.